Modeling the Impact of Climate Change on Hydrological Responses in the Lake Tana Basin, Ethiopia

Achenafi Teklay (achenafi.teklay@gmail.com)
Addis Ababa Science and Technology University
Yihun T. Dile
Texas A & M University
Dereje H. Asfaw
Addis Ababa Institute of Technology
Haimanote K Bayabil
University of Florida
Kibruyesfa Sisay
United Nations Development Programme

Research

Keywords: climate change, streamflow, evapotranspiration, WRF, SWAT, Lake Tana basin

Posted Date: January 2nd, 2020

DOI: https://doi.org/10.21203/rs.2.19829/v1

Version of Record: A version of this preprint was published at Dynamics of Atmospheres and Oceans on November 1st, 2021. See the published version at https://doi.org/10.1016/j.dynatmoce.2021.101278.

Abstract

Background

Hydrologic systems have been changing due to the impact of climate change and climate variability. The impacts of climate change are set to increase in the future due to the rise of global warming. Quantifying the impact of climate change on the spatial and temporal hydrological processes is important for integrated water resource management. The Lake Tana basin, which is the source of the Upper Blue Nile, is vulnerable to climate change and variability. This study was carried out in the four major tributary watersheds of the Lake Tana basin: Gilgel Abay, Gumara, Ribb, and Megech. The climate model and hydrological model was used to (i) to evaluate the performance of the Soil and Water Assessment Tool for study watershed, (ii) to assess the future rainfall and temperature variability and change in the study watershed, and (iii) to examine the impact of climate change on future watershed hydrology. The study used dynamically downscaled climate data for the baseline (2010–2015) and future period (2046–2051) under two Representative Concentration Pathways (RCP4.5 and RCP8.5). The climate scenarios were simulated using the Weather Research and Forecasting (WRF) model, with a 4-km horizontal resolution. A linear scaling method was applied to minimize model biases. The SWAT model was used to estimate the baseline and future hydrology using the bias-corrected climate data.

Results

The performance of the SWAT model was ‘good’ to ‘very good’ for both the calibration and validation periods, with the Nash–Sutcliffe efficiency values between 0.71 to 0.92. The projected changes in rainfall vary with seasons and watershed under both scenarios. On average, annual rainfall may increase by 9.8% and 21.2% under RCP4.5 and RCP8.5 scenarios, respectively. Minimum temperature may rise by 1.68 °C and 2.26 °C while maximum temperature may increase by 1.65 °C and 2.75 °C under RCP4.5 and RCP8.5 scenarios, respectively. The changes in climate may cause an increase in surface runoff by 20.9% and 46.5% under RCP4.5 and RCP8.5 scenarios, respectively, while the evapotranspiration increase by 4.7% and 12.2% under RCP4.5 and RCP8.5, respectively.

Conclusion

The findings provide valuable insights to implement appropriate water management strategies to mitigate and adapt to the negative impacts of climate change and variability on the Lake Tana basin, and other regions which have similar agro-ecology.

1. Background

Climate change is expected to happen due to the anthropogenic alterations of atmospheric composition through the burning of fossil fuels, such as oil and coal, which emit greenhouse gases into the atmosphere (IPCC 2014). Several studies indicated that climate change is one of the most important global environmental challenges to humanity affecting social and ecological systems (Ngongondo et al. 2013; Clifton et al. 2018). The hydrological cycle will be directly altered by the impacts of climate change, subsequently affect local water resource availability in most regions in the world (Faramarzi et al. 2013; Mechal et al. 2015; Li et al. 2016; Aduah et al. 2017; Awal et al. 2018; Jin et al. 2018). However, the magnitude and direction of the impact vary from region to region; for the impact severe to Ethiopia as its economy is rain-fed agriculture, which is highly vulnerable to climate change and variability (Conway and Schipper 2011). Understanding the impacts of climate change is vital especially in regions where the social and ecological systems are highly dependent on climate and water resources such as in Africa.

The potential impacts of climate change and variability on water resources have been studied in different regions in Africa. For example, Faramarzi et al. (2013) analyzed the impact of climate change on freshwater availability in Africa at a coarser resolution for the period of 2020–2040. The results showed that the available water in Africa may increase for entire Africa. Aich et al. (2014) assessed the impact of climate change on streamflow of four large representative African river basins (Niger, Upper Blue Nile, Oubangui and Limpopo basin) and showed a statistically significant increase in streamflow for the period 2070 to 2099 compared to the baseline period of 1970 to 1999. Liersch et al. (2018) also showed that climate change may decrease streamflow of the Upper Blue Nile River for the months June and July, but an increase for the period August to November. Local-scale climate change studies have also been conducted to assess the impacts of climate change and variability on the hydrology of the Upper Blue Nile watersheds (Abdo et al. 2009; Setegn et al. 2011; Dile et al. 2013; Gebre et al. 2015; Nigatu et al. 2016; Abebe and Kebede 2017; Birhan and Worku 2018). For example, Dile et al. (2013) estimated the impact of climate change on streamflow of Gilgel Abay watershed using the SWAT model and downscaled climate data from HadCM3 A2 and B2 scenarios with Statistical Downscaling Tool (SDSM). They found that the mean monthly flow may decrease during the 2010-2040 period and increase during 2070-2100. Recently, Ayele et al. (2016) used a stochastic weather generation approach to downscale climate data from six General Circulation Models (GCMs) for the high (A2) and low (B1) emission scenarios in the Gilgel Abay and Gumara watersheds. The climate data was used as input for the General Water Loading Function (GWLF) hydrological model to simulate runoffs. The results showed that the future

(2020-2039) runoff may increase in both watersheds under all the six GCM outputs. Besides, Melke and Abegaz (2017) estimated the impact of climate change on streamflow in Gumara watershed using SDSM downscaled HadCM3A2a and HadCM3B2a climate outputs in which they found different trends of streamflow between the studied GCMs. Although the studies used different emission scenarios, GCMs, downscaling techniques, and hydrological models, the findings attest that climate change may unequivocally affect the water availability in Africa.

Although there is a consensus that climate change may affect the water resources in the Lake Tana basin, most of the previous studies in the basin assumed empirical-statistical relationships between large-scale predictors (i.e. GCM-derived atmospheric parameters) and local predictands (e.g. rainfall or temperature) (Abdo et al. 2009; Setegn et al. 2011; Dile et al. 2013; Enyew et al. 2014; Ayele et al. 2016). However, the climate has a strong association with local soil conditions, topography, and land use dynamics (Haile et al. 2009; Collow et al. 2014; Cao et al. 2015), which is not properly accounted for in a statistical predictor-predictand relationship. Although most of these concerns are better addressed in the Fifth generation IPCC Assessment Report (IPCC-AR5) Representative Concentration Pathways (RCPs) (van Vuuren et al. 2011; Knutti and Sedláček 2013; Knutti et al. 2013), most of the climate change studies in the Lake Tana basin used GCM based IPCC AR4 Special Report on Emissions Scenarios (SRES). Therefore, estimates from these studies are less reliable since they do not account for local details such as land use, topography, and soil due to the coarse spatial resolution of the GCMs. Although watershed studies in other regions showed that regional climate models (RCMs) provide more reliable results in assessing climate change impacts than GCM-based estimates (Fang et al. 2015; Yhang et al. 2017; Wulong et al. 2018), such studies are lacking in the Lake Tana basin.

This study, therefore, applied a high-resolution RCM with RCP emission scenarios to study the impact of climate change on the hydrology of the Gilgel Abay, Gumara, Ribb, and Megech of the Lake Tana basin. These watershed contribute more than 93% of the inflow to Lake Tana (Kebede et al. 2006). This study is the first of its kind to assess the impact of climate change on the seasonal and annual water resources of the Lake Tana watersheds at finer spatial and temporal resolution. The findings of this study will have paramount importance for the policymakers in Ethiopia since the Lake Tana basin is one of the main growth corridors in the country because of its significance for hydropower generation and irrigation. Besides, the employed methodology can be replicated to investigate the impact of climate change on other basins.

2. Materials And Methods

2.1 Study Area

The study is conducted in the Lake Tana basin, which is located in the Amhara region of Ethiopia (Figure 1). The Lake Tana basin is the headwater of the Upper Blue Nile Basin having a catchment area of ~15,000 km^2. The elevation of the basin ranges between 1780 and 4100 meter above sea level (masl). The Lake Tana, which is the largest freshwater body in Ethiopia, covers 20% of the basin area. Although more than 40 tributary rivers flow into Lake Tana, the major tributaries are Gilgel Abay, Gumara, Ribb, and Megech, which account for more than 93% of the flow to Lake Tana (Kebede et al. 2006). The Gilgel Abay river is the largest tributary that originates from the southern part of the basin and has a catchment area of 4553 km^2 having its outlet at the Lake. The Ribb river is the second largest tributary with a catchment area of 1970 km^2 joining the Lake from east. The Gumara river flows from the eastern part of the basin draining 1780 km^2 of the Lake Tana basin. The Megech watershed is the smallest of the four major tributaries of the Lake Tana basin with a catchment area of 860 km^2. The Megech river joins the Lake Tana from the north.

The climate in the Lake Tana basin is monsoon tropical highland with a rainy season from June to September and a dry season from October to March. The rainfall in the basin differs widely between mean annual rainfall of 800 mm in the northeastern part of the basin and 2000 mm in the southern. The temperature is warmer around Lake Tana with mean annual temperature between 18.6°C and 21.2°C but gets cooler moving away from Lake Tana.

2.2 Modeling Approach

This study involved climate and hydrological modeling to estimate the impact of climate change in the Lake Tana basin. Initially, the quality of all observed climate and streamflow data were checked using basic statistical error checking approaches. Thereafter, the baseline and two future climate scenarios (RCP4.5 and RCP8.5) were dynamically downscaled using the Weather Research and Forecasting (WRF) model. The downscaled climate datasets were corrected from model biases using the linear scaling method. The Soil and Water Assessment Tool (SWAT) model was calibrated and validated using observed climate and streamflow data. Finally, the calibrated and validated SWAT model was used to estimate the baseline and future hydrology using the bias-corrected climate data. The detailed procedures for the climate and hydrologic modeling are presented as follows.

2.2.1 Climate Simulation

Rainfall and temperature datasets of this study were estimated using WRF (version 3.8) regional climate model. The WRF model assumes a fully compressible, and a terrain-following hydrostatic pressure coordinate (Skamarock et al. 2008). The baseline (2010-2015) and two future climate scenarios (2046-2051) were simulated using the model. The baseline dataset was based on a model run using a GCM from the National Centers for Environmental Prediction (NCEP) global FiNaL (FNL), whereas the future scenarios were based on a Community Earth System Model (CESM) participated in phase 5 of the Coupled Model Intercomparison Experiment (CMIP5) (Knutti and Sedláček 2013; Knutti et al. 2013). The NCEP and CMIP5 datasets were selected due to accessibility and spatial resolution. The future scenarios were based on Representative Concentration Pathways (RCPs) from the IPCC fifth assessment report (AR5). This study used RCP4.5 and RCP8.5 emission scenarios. The RCPs are the latest developed climate scenarios, which covers a wider range of futures than those from the SRES (van Vuuren et al. 2011). The RCP4.5 is an intermediate stabilization scenario with an equivalent concentration of carbon dioxide ranging from 580 to 720 ppm in 2100, while the RCP8.5 is a very high emission scenario representing an equivalent concentration of carbon dioxide larger than 1000 ppm in 2100 (IPCC 2014).

This study used the WRF model physical parameterization schemes and model configurations by Teklay et al. (2019). The simulations used nested grids at 36 km, 12 km, and 4 km. The outer domain covers the Indian Ocean, red sea and East Africa region which influence rainfall patterns in Ethiopia (Conway 2000). The inner domain centered at Lake Tana and covers an area of 280 km in the east and 333 km in the north directions. The outer 36 km nest received boundary conditions from the NCEP and CMIP5 fields while the inner 4 km nest was forced at its boundary by the outer and intermediate nests. The three nested domains were run in one-way nesting mode with 35 vertical layers from near the surface to the model top at 50 hPa. The WRF simulation used the Kain-Fritsch cumulus parameterization (Berg et al. 2013), Thompson microphysics (Thompson et al. 2008), Rapid Radiative Transfer Model (RRTMG) for long-wave and shortwave radiation (Hagos et al. 2014), revised MM5 Monin-Obukhov surface layer physics (Jiménez et al. 2012), Noah land surface model (Teklay et al. 2019), and Yonsei University planetary boundary layer physics (Diaz et al. 2015). Due to the shortage of computational resources, the WRF simulations were conducted for six years from 1 January 2010 to 31 December 2015 for the baseline run, and from 1 January 2046 to 31 December 2051 for the future (RCP4.5 and RCP8.5) runs. The simulation outputs were daily rainfall, and daily maximum and minimum temperature at 2 meter above the ground over the respective simulation periods.

Direct application of the RCM outputs for assessing the impact of climate change at the local scale is not recommended due to biases resulting from limitations in the global forcing fields and regional climate models (Hurkmans et al. 2010; Smitha et al. 2018). Therefore, the linear scaling bias correction method was applied to minimize biases from rainfall and temperature data. This method was selected due to its simplicity and satisfactory performance in correcting climatological biases (Fang et al. 2015; Sisay et al. 2017). The baseline rainfall and temperature data were corrected with a multiplier and an additive term on a 10 days' average basis (Fang et al. 2015; Sisay et al. 2017). The correction factors were applied for the future climate of the RCP4.5 and RCP8.5 emission scenarios. The baseline and projected rainfall biases were corrected using Equation 1 and 2, respectively.

$$P_{base,cor} = P_{base,sim} \times \frac{\overline{P}_{obs}}{\overline{P}_{base,sim}} \quad (1)$$

$$P_{proj,cor} = P_{proj,sim} \times \frac{\overline{P}_{obs}}{\overline{P}_{base,sim}} \quad (2)$$

where $P_{base,cor}$ and $P_{proj,cor}$ are the corrected daily rainfall for the baseline and projected period, and $P_{base,sim}$ and $P_{proj,sim}$ are the simulated daily rainfall for the baseline and projected period, and $\overline{P}_{obs}$ and $\overline{P}_{base,sim}$ represent 10 days' average observed and baseline rainfall, respectively.

The baseline temperature is corrected using Equation 3, and projected period temperature is corrected using Equation 4.

$$T_{base,cor} = T_{base,sim} + \left(\overline{T}_{obs} - \overline{T}_{base,sim}\right) \quad (3)$$

$$T_{proj,cor} = T_{proj,sim} + \left(\overline{T}_{obs} - \overline{T}_{base,sim}\right) \quad (4)$$

The subscripts refer to similar meaning as that of the equations in the rainfall correction equations.

To verify the bias correction method and to show the improvement obtained after bias correction, the average daily observation and WRF simulation (before and after bias correction) were compared using statistical measures such as the correlation coefficient (r) and root mean square error (RMSE).

2.2.2 Hydrological Model

The Soil and Water Assessment Tool (SWAT) model was used to assess the impact of climate change on the Gilgel Abay, Gumara, Ribb, and Megech watersheds. The SWAT model is developed to predict the impact of land use, land management practices, and climate change on water balance, nutrient cycling, and sediment transport at a watershed to a river basin and regional scale. It is a physically-based semi-distributed model that functions on a continuous-time step. In the SWAT model, a watershed is divided into sub-basins where each sub-basin will have one or more Hydrologic Response Units (HRUs). HRU is a unique combination of land use, soil, and slope classes. Most of the biophysical processes are calculated at the HRU level and aggregated at the sub-basin level (Neitsch et al. 2011). The SWAT model has been widely applied in the Upper Blue Nile basin and showed satisfactory results (Van Griensven et al. 2012; Dile et al. 2016; Fentaw et al. 2018).

2.2.2.1 Input data

The model requires spatio-temporal data such as topography, land use, soil, weather, and land-management interventions to simulate different processes in the watershed. The model also requires hydrological data (e.g. streamflow) to calibrate and validate the performance of the model. Digital Elevation Model (DEM) is used to delineate the watershed and generate other topographic characteristics. The study used DEM data from the Shuttle Radar Topographic Mission (SRTM), which has a spatial resolution of 90 m. Land use data is required in the SWAT model to define the HRUs and link the landscape with the crop database. The land use data was produced from 30 m Landsat image using a supervised classification method for the 2016 Ethiopia land cover (Figure 2). The classification was satisfactory with an overall accuracy of 87.9% and a Kappa coefficient of 0.79 (Kindu et al. 2013). The original raw data was obtained from the Regional Centre for Mapping of Resources for Development. The soil data was used to create HRUs and provide physiochemical information about the soils in the landscape. The soil map was obtained from the Ethiopian Ministry of Water, Irrigation and Electricity (EMWIE). The physical and chemical soil properties required by the SWAT model were extracted from the International Soil Reference and Information Center. Daily rainfall, minimum/maximum temperature, solar radiation, wind speed and humidity data are required to simulate processes in the SWAT model. Climate data within and around the Lake Tana basin were collected from the Ethiopian National Meteorology Services Agency. The rainfall and temperature data were available for 27 climatic stations (Figure 1) for the period 1982 to 2015. Missing values in climate data were filled using the SWAT built-in weather generator. Streamflow data is often used to calibrate and validate the performance of the SWAT model. This study used monthly streamflow data of Gilgel Abay, Gumara, Ribb and Megech for model calibration and validation. Observed daily and monthly streamflow data for the period 1990-2015 was obtained from the EMWIE.

2.2.2.2 SWAT model setup, calibration and validation

The watershed boundary was delineated by considering the hydrometer station as an outlet (Figure 1). The watershed was discretized using a threshold area of 25 km^2, which provided 31, 26, 27, 15 sub-basins for Gilgel Abay, Gumara, Ribb, and Megech watersheds, respectively. The HRUs were defined using accounting all the slope, land use, and soil features in the sub-basins. Angereb reservoir is located in the Megech watershed, which was included in the SWAT model setup. Angereb dam was constructed in 1997 to supply potable water to Gondar town (Haregeweyn et al. 2012). The reservoir has a total area of 50 ha and 60 ha at its principal spillway and emergency spillway, respectively. The volume of the reservoir at the principal and emergency spillway is 3,530,000 m^3 and 5,160,000 m^3, respectively. SWAT has several options to simulate biophysical processes. The surface runoff was estimated using the Soil Conservation Service Curve Number (SCS CN) method (Betrie et al. 2011; Fentaw et al. 2018). Flow within the channels was routed using variable storage method. The evapotranspiration was estimated using the Penman- Monteith method (Gebre and Ludwig 2015).

The model parameters were calibrated using the Sequential Uncertainty Fitting version 2 (SUFI-2) in the SWAT-CUP (SWAT Calibration and Uncertainty Program) (Abbaspour et al. 2004). The models were calibrated and validated using observed monthly streamflow data at the Gilgel Abay, Gumara, Ribb, and Megech river gauging stations (Figure 1). The calibration and validation were conducted for the periods 1900–2004 and 2005–2015, respectively. The model was warm-up for three years (1987-1989) to properly initiate the biophysical processes. The model calibration considered 18 hydrological parameters (Table 1), which were selected based on the literature (Setegn et al. 2008; Gebremicael et al. 2013; Dile et al. 2016; Halefom et al. 2018; Teklay et al. 2018).

2.3 Model Evaluation

Model performance was evaluated by comparing the observed and simulated streamflow using the Nash-Sutcliffe efficiency (NSE) and percent bias (PBIAS). The NSE is a normalized statistic that estimates the relative magnitude of the residual variance compared to the observed data variance (Nash and Sutcliffe 1970). PBIAS compares the average tendency of the simulated data to the corresponding observed data (Gupta et al. 1999). The NSE value theoretically ranges from negative infinity to 1; a value of 1 corresponds to a perfect match between observed and simulated values (Nash and Sutcliffe 1970). While the PBIAS value can be positive or negative, in which a value of zero represents the best model simulation performance (Moriasi et al. 2007). A positive PBIAS value indicates model underestimations, and a negative value indicates model overestimations. The NSE and PBIAS are computed using Equation 5 and 6, respectively. Moriasi et al. (2007) suggested that a model simulation that provides an NSE value of >0.5 and PBIAS value of is considered as satisfactory.

$$NS = 1 - \left(\sum_{i=1}^{N} (X_{obs} - X_{sim})^2 / \sum_{i=1}^{N} (X_{obs} - \bar{X})^2 \right) \quad 5$$

$$PBIAS = \left(\sum_{i=1}^{N} (X_{obs} - X_{sim}) / \sum_{i=1}^{N} X_{obs} \right) * 100 \quad 6$$

where, X_{obs} is the observed streamflow data, X_{sim} is the simulated streamflow data, $\bar{X}$ is the mean of the observed streamflow data, and N is the total number of streamflow data.

The uncertainty of the simulations was estimated using a p-factor and r-factor (Abbaspour et al. 2007). The p-factor measures percent of observed data bracketed by the 95% prediction uncertainty (95PPU). While the r-factor measures the thickness of the uncertainty band. It is estimated by dividing the average thickness of the 95PPU band by the standard deviation of the observed data. The p-factor value ranges between 0 and 1, while the r-factor ranges between 0 and infinity. A p-factor of 1 and r-factor of 0 represent a simulation that exactly matches the observed data. According to Abbaspour et al. (2007), a model providing a p-factor ≥ 0.75 and r-factor ≤ 1.5 is considered robust for streamflow simulation.

3. Results

3.1 Bias Correction of Climate Variable

Daily rainfall and temperature data were extracted from the grid-based WRF simulations using coordinates of the 27 meteorological stations (Figure 1). Figure 3 shows observed and WRF simulated rainfall and temperature data, averaged over the Lake Tana basin, for the baseline period (2010 – 2015). The WRF model without bias correction performed well in simulating rainfall only during the dry season (January to May); while it considerably overestimated rainfall during the rainy season (June to September) (Figure 3a). Besides, the model showed consistent cold biases of maximum temperature (Tmax) across all the months (Figure 3b), while it overestimated minimum temperature (Tmin) values most of the time (Figure 3c). These results highlighted the need for bias correction, and it improved the WRF model's outputs considerably. Cold and warm biases of maximum and minimum temperatures, respectively were substantially reduced. Similarly, the bias-corrected WRF model (WRF-BC) reproduced monthly rainfall very well except for slight overestimations during the rainy months of July and August.

While bias correction improved overall performances of the WRF model in simulating rainfall and temperature; there were differences in the model evaluation statistics (Table 2). For temperature, bias-corrected values were very close to the observed. After bias correction, the average cold bias was substantially reduced from 1.42 ºC to 0.02 ºC for maximum temperature and the warm bias decreased from 1.45 ºC to 0.03 ºC for minimum temperature (Table 2). Moreover, the RMSE was considerably reduced by 1.27 ºC and 1.36 ºC for maximum and minimum temperatures, respectively. However, RMSE for rainfall was decreased from 5.43 to 3.88 mm/day. In addition, bias-corrected simulations showed good agreement with the observed data. Correlations between observed and simulated data were improved from 0.65, 0.76, and 0.60 to 0.78, 0.89, and 0.84 for rainfall, maximum and minimum temperatures, respectively. These results suggest that bias correction output is acceptable and consistent with the previous studies (Gebre and Ludwig 2015; Sisay et al. 2017; Goshime et al. 2019).

3.2 Projected Rainfall and Temperature

3.2.1 Projected temperature

Temperature projections using the WRF model were averaged by season to investigate overall trends of future climate in Gilgel Abay, Gumara, Ribb, and Megech watersheds. The baseline (2010 – 2015) and projected (2046 - 2051) seasonal temperature distributions for the four

watersheds are presented in Figure 4. The baseline and projected minimum and maximum temperatures show the same seasonal pattern. The simulated maximum temperature is high during spring, whereas minimum temperature is high during summer. Compared to the baseline period, both RCP4.5 and RCP8.5 seasonal maximum and minimum temperatures were predicted to increase in all the watersheds. In the Gilgel Abay watershed, the mean annual maximum temperature is projected to increase by 1.64 °C and 2.76 °C under RCP4.5 and RCP8.5 scenarios, respectively, while minimum temperature is expected to increase by 1.65 °C under the RCP4.5 and 2.16 °C under the RCP8.5. The seasonal increase in maximum temperature showed a large variation with a range from 0.28 °C to 3.19 °C under RCP4.5 and 1.98 °C to 3.48 °C under RCP8.5 (Figure 4a). The maximum temperature increase is projected to be higher during autumn under both scenarios (Figure 4a). However, the minimum temperature change during summer is projected to be as high as 2.17 °C and 3.12 °C under RCP4.5 and RCP8.5 scenarios, respectively (Figure 4b). In the Gumara watershed, the mean annual maximum temperature is projected to increase by 1.85 °C and 2.94 °C and minimum temperature by 1.77 °C and 2.33 °C under RCP4.5 and RCP8.5, respectively. The seasonal increase in maximum temperature displayed a large variation with a range from 0.63 °C to 3.23 °C for RCP4.5 and 2.05 °C to 3.84°C for RCP8.5 (Figure 4c). The highest minimum temperature increase is projected to occur in summer with 2.16 °C and 3.15 °C for RCP4.5 and RCP8.5 projections, respectively (Figure 4d). In the Ribb watershed, the mean annual maximum temperature increase by 1.49 °C and 2.67 °C and minimum temperature by 1.66 °C and 2.25 °C under RCP4.5 and RCP8.5, respectively. Compared to the baseline period, the RCP4.5 maximum temperature seasonal increase is projected between 0.19 °C and 3.02 °C, while under RCP8.5 between 1.62 °C and 3.65 °C (Figure 4e). The simulated minimum temperature under RCP4.5 did not show considerable variation among seasons (Figure 4f). In the Megech watershed, the mean annual maximum temperature is projected to increase on average by 1.62 °C and 2.63 °C while the average increase in minimum temperature is projected to increase by 1.63 °C and 2.28 °C under RCP4.5 and RCP8.5, respectively. The seasonal maximum temperature increase is expected to vary between 0.30 °C to 3.18 °C and 1.85 °C to 3.60 °C under for RCP4.5 and RCP8.5, respectively (Table 4g).

3.2.1 Projected rainfall

The seasonal distributions of rainfall under the two scenarios were similar to the baseline period with the highest rainfall (705 - 1547 mm) occurring during summer while the smallest rainfall (4 – 33 mm) is during winter (Figure 5). The mean annual rainfall under RCP4.5 and RCP8.5 scenarios are projected to be higher than the baseline period. Similar to temperature, simulation of rainfall under RCP8.5 is expected to be substantially greater than the RCP4.5 simulations in most of the watersheds. Under RCP8.5, the mean annual rainfall is projected to increase by 668 mm, 337 mm, 275 mm, and 33.9 mm in Gilgel Abay, Gumara, Ribb, and Megech watersheds, respectively. The greatest increase (34.6%) is expected in Gilgel Abay watershed, while Megech watershed could experience the smallest increase (3%) under both scenarios. As shown in Figure 5, Megech watershed receives the smallest mean annual rainfall in the future.

On a seasonal scale, the rainfall under RCP8.5 is larger than the baseline values during most seasons. In the Gilgel Abay watershed, rainfall is projected to increase during all four seasons (Figure 5a). The increases in rainfall under RCP4.5 and RCP8.5 are expected to occur during spring (up to 83.4%) and autumn (up to 63.4%), respectively. In the Gumara watershed, the seasonal rainfall is projected to increase by up to 180% and 74.2% under the RCP4.5 and RCP8.5, respectively (Figure 5b). However, the rainfall under RCP4.5 may decrease by 18.7% and 28.3% during summer and winter, respectively. In the Ribb watershed, rainfall is projected to increase during spring under both scenarios. The rainfall under RCP4.5 may decrease by 165.7 mm and 85.9 mm during summer and autumn, respectively. On the contrary, the rainfall under RCP8.5 may increase by 59.7 mm and 93.3 mm during summer and autumn, respectively (Figure 4c). In the Megech watershed, rainfall may increase by 133.5% and 28.4% in spring under RCP4.5 and RCP8.5, respectively, but rainfall during summer may slightly decrease under both scenarios (Figure 4d).

3.3 SWAT Model Calibration and Validation

Statistical analysis of the SWAT model results indicates that the monthly streamflow was well simulated for most of the calibration period, with NSE > 0.72 for each watershed and PBIAS well within the satisfactory range of ±25% according to Moriasi et al. (2007) (Table 3). Evaluation of the average monthly streamflow during calibration revealed that the SWAT model overestimated the streamflow in the Gilgel Abay, Ribb, and Megech watershed by 1.1%, 15.4%, and 15.1%, respectively, while the model underestimated the flow in the Gumara watershed by about 10.1%. The agreement between observed and simulated flow was slightly better for the Gilgel Abay and Gumara watersheds, compared to the Ribb and Megech watersheds. Validation results also showed overall very good model performances in all watersheds, with NSE values > 0.75 and PBIAS < ±10 (Table 3). During the validation period, the SWAT model slightly overestimated average streamflow by about 6.1%, 7.2%, and 8.3% in the Gilgel Abay, Gumara, and Ribb watersheds, respectively, whereas it underestimated the stream flow by about 8.4% in Megech watershed.

The uncertainty bands of the model captured most of the observed streamflow with p-factor > 0.82 for Gilgel Abay and Gumara watersheds. The 95PPU relative width was slightly small (0.75-0.78) in Megech and Ribb watersheds, but it was under the acceptable model estimates (Abbaspour et al. 2007). Overall, model simulation results demonstrated that the calibrated and validated model replicated observed streamflow very well in all study watersheds (Moriasi et al. 2007; Arnold et al. 2012). Our findings are in agreement with previous studies in the

region (Dile et al. 2016; Halefom et al. 2018; Teklay et al. 2018). Therefore, it is safe to conclude that the SWAT model is reliable to simulate the watershed hydrological processes in the Ethiopian highlands.

Moreover, the graphical comparison results showed that simulated streamflow was in a very good agreement with observations at the four gauging stations (Figure 6). However, the model tends to underestimate peak flows while overestimating low flows depending on the study watershed. The majority of the peak events were not captured adequately over the study watersheds owing to the poor performance of the SWAT model for peak flow simulations (Polanco et al. 2017; Lee et al. 2018).

3.4 The Impacts of Climate Change on Hydrological Responses

The major hydrological components were simulated using the calibrated SWAT model and bias-corrected climate date. The simulated hydrological components for the projected period (2046-2051) under RCP4.5 and RCP8.5 scenarios were compared to the corresponding values in the baseline period (2010–2015). Overall, the mean annual rainfall, streamflow, and evapotranspiration are projected to increase compared to the baseline period in all the four study watersheds (Table 4). The magnitude and direction of seasonal streamflow and evapotranspiration changes were different among watersheds except for Gumara and Ribb.

In the Gilgel Abay watershed, Overall, the mean annual streamflow may increase by 38.9% and 58.2%, which corresponds to 22.1% and 34.7% increases in rainfall under RCP4.5 and RCP8.5 scenarios, respectively (Table 4). On a seasonal scale, the streamflow under RCP4.5 and RCP8.5 is projected to increase in all seasons except for winter (Figure 7a). The streamflow changes were mostly related to rainfall change over the watershed. Under RCP8.5, the changes in summer rainfall clearly showed the largest increases (337 mm) in comparison to other seasons (Figure 5a), with a maximum streamflow increase of 245 mm during summer. Similarly, the RCP4.5 autumn rainfall increase by 131 mm (30.3%), thereby considerably increasing streamflow by 180 mm (61.2%). However, the winter season streamflow is projected to decrease slightly (2.9 mm) under RCP4.5, despite projected increases in rainfall during the same time, since the rainfall increase substantially contributed to soil moisture increase (Table S2). The mean annual evapotranspiration under RCP8.5 is expected to increase by 10.7% due to the average temperature increase of 2.5 °C and rainfall increase of 34.7%. However, the mean annual evapotranspiration under RCP4.5 shows only a marginally increase (0.1%). The evapotranspiration may increase in spring and summer under both emission scenarios. This may be due to the increase in average temperature and rainfall in these seasons. Although the temperature increase may occur in winter, evapotranspiration may decrease by 7.1 mm (14.1%) and 15.8 mm (31.1%) under RCP4.5 and RCP8.5 scenarios, respectively. These results indicated that all the temperature increases may not contribute to evapotranspiration increases.

As can be seen in Figure 7, the direction of hydrologic response changes in Gumara and Ribb watersheds were similar, since the hydrologic model in both watersheds used almost the same meteorological stations that are located in the eastern part of the Lake Tana basin (Figure 1). Therefore, the results of the Gumara watershed are presented here for clarity purposes. The mean annual streamflow increase under RCP4.5 is very small (0.1%), while the mean annual streamflow increase under RCP8.5 is considerable large (26.7%). This may be due to a larger increase mean annual rainfall under RCP8.5 than under RCP4.5. Under RCP4.5, the streamflow is projected to decrease in most season, with the largest decrease of 141.5 mm (26.1%) during summer. However, the streamflow increase during spring is extremely large (195.2 mm), which may cause flooding. The RCP8.5 streamflow may increase in all seasons with a range between 33.8 mm (195.5%) during spring and 158 mm (29.2%) during summer. Such considerable increases were driven by projected increases in rainfall during summer (126.4 mm). The mean annual evapotranspiration is projected to increase by 9.6% and 16.5% under RCP4.5 and RCP8.5 scenarios, respectively, which corresponds with the projected increases in average annual temperature by 1.81 °C and 2.64 °C and rainfall by 3.9% and 22.1%, under RCP4.5 and RCP8.5, respectively (Table 4). The RCP4.5 projections show reductions in evapotranspiration during summer and autumn, while the RCP8.5 scenarios show increases in evapotranspiration during all four seasons except for winter.

In the Megech watershed, the mean annual streamflow may increase in the future period under both scenarios. Unlike other watersheds, the projected increase in streamflow under RCP4.5 is slightly greater than under RCP8.5. This could be due to the grater temperature increases under RCP8.5 (0.84 °C more than RCP4.5) while rainfall was more or less the same (Table 4), which results in greater evapotranspiration under RCP8.5. The streamflow projection under both scenarios may increase in all seasons except for winter (Figure 7d). The streamflow projections show the largest increase during spring under RCP4.5 and during summer under RCP8.5. The mean annual evapotranspiration increase by 1.7% and 8.9% under RCP4.5 and RCP8.5 scenarios, respectively. The evapotranspiration, however, is expected to decrease during winter and autumn under both scenarios.

4. Discussion

The Lake Tana basin is one of the growth corridors in Ethiopia where large and small scale irrigation and hydropower projects are under construction. Many studies have indicated that climate change has a substantial impact on streamflow from the major tributaries of the Lake Tana basin, and the studies have suggested that the streamflow variability of tributary rivers was the result of rainfall variability and

temperature increase. These studies used rainfall and temperature output from coarse spatial resolution. However, few studies have evaluated the impact of climate change on streamflow response in the major tributaries rivers of the Lake Tana basin using dynamically downscaled climate data.

The projected mean annual maximum and minimum temperatures under RCP4.5 and RCP8.5 scenarios are higher than the baseline period. The mean annual temperature increase under RCP8.5 is considerably larger than that under RCP4.5 because the RCP8.5 scenario represents a higher radiative forces (Wulong et al. 2018). The climate projections results showed that overall warming over the Lake Tana basin, with an average temperature increase of 1.66 °C and 2.50 °C under RCP4.5 and RCP8.5 scenarios, respectively. These results are comparable with the previous studies (Dile et al. 2013; Nigatu et al. 2016; Liersch et al. 2018; Mekonnen and Disse 2018) in the Upper Blue Nile basin. Besides, the results agree with the study by Ayele et al. (2016) in Gilgel Abay and Gumara watersheds. They reported that projected (2020-2039) temperature in the A2/B2 scenarios will increase by 1.2/1.1°C and 0.8/0.7°C in Gilgel Abay and Gumara watershed, respectively. The simulated mean annual rainfall under RCP4.5 and RCP8.5 is larger than the baseline period. The result showed that the RCP4.5 rainfall simulation increased rates were greater in spring than other seasons, which is in agreement with Worqlul et al. (2018) findings in the Upper Blue Nile basin. Moreover, rainfall under RCP8.5 is expected to increase in all four seasons in all the watersheds. These results are in agreement with results from previous studies in the Lake Tana basin (Gebre and Ludwig 2015; Ayele et al. 2016; Nigatu et al. 2016; Melke and Abegaz 2017), though variations exist in the magnitude of change, which could be due to differences in GCM models, emission scenarios, and downscaling methods used between studies. However, this result contradicted with the study by Setegn et al. (2011) in the Lake Tana basin who reported decreasing trends in future rainfall. A decrease in seasonal rainfall in Gumara, Ribb, and Megech watershed resemble with the results by Beyene et al. (2010), who also showed a decrease in the mean monthly rainfall in 2040-2069 in Nile river basin, where our study watersheds are located.

Several researchers (Dile et al. 2013; Gebre and Ludwig 2015; Ayele et al. 2016) have shown that the streamflow and evapotranspiration were projected to increase in the major tributary rivers in the Lake Tana basin, and this is very similar to the results of this study. The seasonal streamflow variation mainly associated with seasonal rainfall variation. However, the streamflow increase rate was larger than the rainfall increases rate, which is consistent with the findings of Aich et al. (2014) from four African River basins. They reported that a 25% increase in rainfall leads to a 50% increase in the river discharge over Upper Blue Nile Basin. The increase in streamflow due to rainfall increment was also discussed by Pandey et al. (2017); they revealed that a 28% increase in annual rainfall may result in streamflow increased by approximately 49% from their study in the Armur watershed in Godavari river basin, India. The decrease in streamflow during the rainy season associated with the rainfall reduction corresponds with the findings of Worqlul et al. (2018) in the Upper Blue Nile Basin, Ethiopia. This highlights climate variation during the rainy season could have a profound effect on the annual hydrological responses. Although the rainfall under RCP4.5 slightly decreases during summer and autumn, the streamflow did not show a reduction trend in these seasons. This could be due to the excess soil moisture in the previous season (i.e. during spring, RCP4.5 soil moisture increase by 67.4 mm Table S2). Similar findings were reported in the Upper Blue Nile Basin(Roth et al. 2018) and Northern Lake Erie Basin in Canada (Zhang et al. 2018). The evapotranspiration was expected to increase at rates similar to those of the temperature and rainfall dynamics, which is in agreement with findings (Gebre and Ludwig 2015; Lemann et al. 2017; Teklesadik et al. 2017; Birhan and Worku 2018) in the Upper Blue Nile Basin. The evapotranspiration, however, is expected to decrease during winter under RCP8.5, contrary to most of the studies conducted in the surrounding watersheds (Enyew et al. 2014; Ayele et al. 2016).

Although the climate variables were simulated using the RCM and updated emission scenarios, there are several uncertainties associated with the climate and hydrological models. Both hydrological and climate model simulations have not considered land-use dynamics; but land use has a significant role in the partitioning of the hydrologic components into infiltration, interception, and evapotranspiration (Wagner et al. 2016; Marhaento et al. 2018; Sunde et al. 2018; Woldesenbet et al. 2018). Besides, land use dynamics will directly influence the land surface-atmosphere interaction and consequently alter the climate processes and patterns (Deng et al. 2013). Therefore, future studies should consider the combined impact of climate and land use change on hydrological responses. Moreover, climate simulation should incorporate a very fine spatial resolution to resolve the complex topography.

5. Conclusion

This study assessed the response of hydrological processes in four major tributaries of Lake Tana basin (Gilgel Abay, Gumara, Ribb, and Megech watershed) to a possible future climate change scenario using the WRF model and a physical distributed hydrological model (SWAT). Overall, WRF simulations reproduced average monthly observation but large biases were found in some cases. The linear scaling bias correction method was capable of correcting most biases with the WRF model. Climate projection showed that rainfall and temperature may increase in the mid-21st century (2046-2051) in all the four study watersheds. Compared to the baseline period (2010-2015), the average temperature is likely to increase by 1.66 °C and 2.50 °C under the RCP4.5 and RCP8.5 scenarios, respectively. Similarly, the mean annual rainfall is likely to increase by 9.8% and 21.1% under the RCP4.5 and RCP8.5 scenarios, respectively.

In all the watersheds, the mean annual streamflow is predicted to increase by 0.1 – 38.9% and 4 - 58.2% under RCP4.5 and RCP8.5 scenarios, respectively, which implies that the overall amount of the water resources may not decrease in the future period over the Lake Tana basin. However, streamflow seasonal variation is large under both scenarios in all four watersheds. Projected annual evapotranspiration in the watersheds will vary on average from 0.1 to 9.6% under RCP4.5 and 8.9 to 16.5% under RCP8.5. While the magnitude and direction of the changes of streamflow and evapotranspiration can vary, impacts of climate change on water resources in the Lake Tana basin need to be taken in to account for future water resources planning. Moreover, the results obtained from this modeling study provide critical insights, potentially helping resource managers and government policymakers to develop effective water resource management strategies in the face of climate change. Based on the results, flood controlling practices should be considered in Gilgel Abay watershed because streamflow may increase by 245 mm (46.1%) during the main rainy season. In the Gumara and Ribb watersheds, a considerable amount of streamflow is expected to occur during spring which could be used to support irrigation practices. However, the projected climate and hydrologic components of Megech watershed highlight the need to put in place appropriate adaptation measures to meet the future water demand for domestic and agricultural production.

Abbreviations

WRF: Weather Research and Forecasting; GCMs: General Circulation Models; RCMs: regional climate models; NCEP FNL: National Centers for Environmental Prediction Global FiNaL; CESM; Community Earth System Model; CMIP5: Climate Model Intercomparison Project 5; RCPs: Representative Concentration Pathways; RRTMG: Rapid Radiative Transfer Model; HRUs: Hydrologic Response Units; DEM: Digital Elevation Model; SRTM; Shuttle Radar Topographic Mission; EMWIE: Ethiopian Ministry of Water, Irrigation and Electricity; SWAT: Soil and Water Assessment Tool; SDSM: Statistical Downscaling Tool; SWAT-CUP: Soil and Water Assessment Tool Calibration and Uncertainty Programs; NSE: Nash-Sutcliffe efficiency.

Declarations

Authors' contributions

AT, DA, and YD developed study concept and design. AT and KS did data collection, processing, analysis and interpretation of data. AT, YD and HB prepared all figures and wrote the manuscript. All authors read and approved the final manuscript.

Author information

[1] Ethiopian Institute of Water Resources, Department of Water Resources Engineering and Management, Addis Ababa University, Addis Ababa, Ethiopia. [2] Spatial Science Laboratory, Ecosystem Science and Management Department, Texas A & M University, College Station, TX, 77801, USA. [3] Addis Ababa Institute of Science and Technology, School of Environmental and Civil Engineering, Addis Ababa University, Addis Ababa, Ethiopia. [4] Agricultural and Biological Engineering, Tropical Research and Education Center, Institute of Food and Agricultural Sciences, University of Florida, Homestead, FL, 33031, USA. [5] United Nations Development Programme, Addis Ababa, Ethiopia.

Acknowledgements

The National Meteorological Agency of Ethiopia is gratefully acknowledged for providing rainfall and temperature data. We also acknowledge the financial and software support provided by the University of Gondar and Addis Ababa University.

Competing interests

The authors declare that they have no competing interests.

Availability of data and materials

Land use data was obtained obtained from the Regional Centre for Mapping of Resources for Development (RCMRD) at https://geoportal.rcmrd.org. Soil data was downloaded from the FAO Harmonized global soils database at http://www.waterbase.org/download_data.html. The CMIP5 boundary data for the WRF model were sourced at http://rda.ucar.edu/datasets/ds083.2. The CMIP5 boundary data for the WRF model were sourced at http://rda.ucar.edu/datasets/ds316.1.
The streamflow and station weather data were provided by Ethiopian Ministry of Water, Irrigation and Electricity and Ethiopian National Meteorology Services Agency on official request, and cannot be shared publicly without their consent.

Consent for publication

Not applicable.

Ethics approval and consent to participate

Not applicable.

Funding

This research was funded by Addis Ababa University post graduate program and university of Gondar research and community service.

References

Abbaspour K, Johnson C, van Genuchten M (2004) Estimating Uncertain Flow and Transport Parameters Using a Sequential Uncertainty Fitting Procedure. Vadose Zo J 3:1340–1352

Abbaspour KC, Yang J, Maximov I, et al (2007) Modelling hydrology and water quality in the pre-alpine/alpine Thur watershed using SWAT. J Hydrol 333:413–430. https://doi.org/10.1016/j.jhydrol.2006.09.014

Abdo KS, Fiseha BM, Rientjes THM, et al (2009) Assessment of climate change impacts on the hydrology of Gilgel Abay catchment in Lake Tana basin, Ethiopia. Hydrol Process 23:3661–3669. https://doi.org/10.1002/hyp.7363

Abebe E, Kebede A (2017) Assessment of Climate Change Impacts on the Water Resources of Megech River. Open J Mod Hydrol 7:141–152. https://doi.org/10.4236/ojmh.2017.72008

Aduah MS, Jewitt GPW, Toucher MLW (2017) Scenario-based impacts of land use and climate changes on the hydrology of a lowland rainforest catchment in Ghana , West Africa. Hydrol Earth Syst Sci

Aich V, Liersch S, Vetter T, et al (2014) Comparing impacts of climate change on streamflow in four large African river basins. Hydrol Earth Syst Sci 18:1305–1321. https://doi.org/10.5194/hess-18-1305-2014

Arnold JG, Moriasi DN, Gassman PW, et al (2012) SWAT: Model Use, Calibration, and Validation. Trans ASABE 2012 55:1491–1508

Awal R, Fares A, Bayabil H (2018) Assessing potential climate change impacts on irrigation requirements of major crops in the brazos headwaters Basin, Texas. Water (Switzerland) 10:1–15. https://doi.org/10.3390/w10111610

Ayele HS, Li M-H, Tung C-P, Liu T-M (2016) Assessing Climate Change Impact on Gilgel Abbay and Gumara Watershed Hydrology, the Upper Blue Nile Basin, Ethiopia. Terr Atmos Ocean Sci 27:1005–1018. https://doi.org/10.3319/tao.2016.07.30.01

Berg LK, Gustafson WI, Kassianov EI, Deng L (2013) Evaluation of a Modified Scheme for Shallow Convection: Implementation of CuP and Case Studies. Mon Weather Rev 141:134–147. https://doi.org/10.1175/MWR-D-12-00136.1

Betrie G, Mohamed Y, Van Griensven A, Srinivasan R (2011) Sediment management modelling in the Blue Nile Basin using SWAT model. Hydrol Earth Syst Sci 15:807–818. https://doi.org/10.5194/hess-15-807-2011

Beyene T, Lettenmaier DP, Kabat P (2010) Hydrologic impacts of climate change on the Nile River Basin: Implications of the 2007 IPCC scenarios. Clim Change 100:433–461. https://doi.org/10.1007/s10584-009-9693-0

Birhan MW, Worku FA (2018) Impact of climate change and variability in the hydrology of chokie mountain basin, Ethiopia. Int J Eng Manafement Sci 9:44–51

Cao Q, Yu D, Georgescu M, et al (2015) Impacts of land use and land cover change on regional climate : a case study in the agro-pastoral transitional zone of China Impacts of land use and land cover change on regional climate : a case study in the agro-pastoral transitional zone of China. Environ Res Lett 10:1–12. https://doi.org/doi:10.1088/1748-9326/10/12/124025

Clifton CF, Day KT, Luce CH, et al (2018) Effects of climate change on hydrology and water resources in the Blue Mountains, Organ, USA. Clim Serv 1–11. https://doi.org/10.1016/j.cliser.2018.03.001

Collow TW, Robock A, W. Wu (2014) Influences of soil moisture and vegetation on convective precipitation forecasts over the United States Great Plains. J Geophys Res Atmos 119:9338–9358. https://doi.org/10.1002/2014JD021454.Received

Conway D (2000) The climate and hydrology of the Upper Blue Nile river. Geogr J 166:49–62. https://doi.org/10.1111/j.1475-4959.2000.tb00006.x

Conway D, Schipper ELF (2011) Adaptation to climate change in Africa: Challenges and opportunities identified from Ethiopia. Glob Environ Chang 21:227–237. https://doi.org/10.1016/j.gloenvcha.2010.07.013

Deng X, Zhao C, Yan H (2013) Systematic Modeling of Impacts of Land Use and Land Cover Changes on Regional Climate: A Review. Adv Meteorol 2013:1–11. https://doi.org/doi.org/10.1155/2013/317678

Diaz JP, González a., Expósito FJ, et al (2015) WRF multi-physics simulation of clouds in the African region. Q J R Meteorol Soc 141:2737–2749. https://doi.org/10.1002/qj.2560

Dile YT, Berndtsson R, Setegn SG (2013) Hydrological Response to Climate Change for Gilgel Abay River, in the Lake Tana Basin - Upper Blue Nile Basin of Ethiopia. PLoS One 8:1–13. https://doi.org/10.1371/journal.pone.0079296

Dile YT, Daggupati P, George C, et al (2016) Introducing a new open source GIS user interface for the SWAT model. Environ Model Softw 85:129–138. https://doi.org/10.1016/j.envsoft.2016.08.004

Enyew B, Lanen H Van, Loon A Van (2014) Assessment of the Impact of Climate Change on Hydrological Drought in Lake Geology & Geosciences Assessment of the Impact of Climate Change on Hydrological Drought in. Geol Geosci 3:1–18. https://doi.org/10.4172/2329-6755.1000174

Fang GH, Yang J, Chen YN, Zammit C (2015) Comparing bias correction methods in downscaling meteorological variables for a hydrologic impact study in an arid area in China. Hydrol Earth Syst Sci 19:2547–2559. https://doi.org/10.5194/hess-19-2547-2015

Faramarzi M, Abbaspour KC, Ashraf Vaghefi S, et al (2013) Modeling impacts of climate change on freshwater availability in Africa. J Hydrol 480:85–101. https://doi.org/10.1016/j.jhydrol.2012.12.016

Fentaw F, Mekuria B, Arega A (2018) Impacts of Climate Change on the Water Resources of Guder Catchment, Upper Blue Nile, Ethiopia. Waters 1:16–29. https://doi.org/10.31058/j.water.2018.11002

Gebre SL, Ludwig F (2015) Hydrological Response to Climate Change of the Upper Blue Nile River Basin: Based on IPCC Fifth Assessment Report (AR5). J Climatol Weather Forecast 03:1–15. https://doi.org/10.4172/2332-2594.1000121

Gebre SL, Tadele K, Mariam BG (2015) Potential Impacts of Climate Change on the Hydrology and Water resources Availability of Didessa Catchment, Blue Nile River Basin, Ethiopia. J Geol Geosci 04:1–7. https://doi.org/10.4172/2329-6755.1000193

Gebremicael TG, Mohamed Y a., Betrie GD, et al (2013) Trend analysis of runoff and sediment fluxes in the Upper Blue Nile basin: A combined analysis of statistical tests, physically-based models and landuse maps. J Hydrol 482:57–68. https://doi.org/10.1016/j.jhydrol.2012.12.023

Goshime DW, Absi R, Ledésert B (2019) Evaluation and Bias Correction of CHIRP Rainfall Estimate for Rainfall-Runo ff Simulation over Lake. Hydrology 6:1–22

Gupta H, Sorooshian S, Yapo P (1999) Status of Automatic Calibration for Hydrological Models: Comparsion with Multilevel Expert Calibration. J Hydrol Eng 4:135–143

Hagos S, Leung LR, Xue Y, et al (2014) Assessment of uncertainties in the response of the African monsoon precipitation to land use change simulated by a regional model. Clim Dyn 43:2765–2775. https://doi.org/10.1007/s00382-014-2092-x

Haile AT, Rientjes T, Gieske A, Gebremichael M (2009) Rainfall variability over mountainous and adjacent lake areas: The case of Lake Tana basin at the source of the Blue Nile River. J Appl Meteorol Climatol 48:1696–1717. https://doi.org/10.1175/2009JAMC2092.1

Halefom A, Sisay E, Worku T, et al (2018) Precipitation and Runoff Modelling in Megech Watershed , Tana Basin , Amhara Region of Ethiopia. 8:45–53. https://doi.org/10.5923/j.ajee.20180803.01

Haregeweyn N, Melesse B, Tsunekawa A, et al (2012) Reservoir sedimentation and its mitigating strategies : a case study of Angereb reservoir (NW Ethiopia). J Soils Sediments 12:291–305. https://doi.org/10.1007/s11368-011-0447-z

Hurkmans R, Terink W, Uijlenhoet R, et al (2010) Changes in streamflow dynamics in the Rhine basin under three high-resolution regional climate scenarios. J Clim 23:679–699. https://doi.org/10.1175/2009JCLI3066.1

IPCC (2014) Climate Change 2014. Synthesis Report:

Jiménez PA, Dudhia J, González-Rouco JF, et al (2012) A Revised Scheme for the WRF Surface Layer Formulation. Mon Weather Rev 140:898–918. https://doi.org/10.1175/MWR-D-11-00056.1

Jin J, Wang G, Zhang J, et al (2018) Impacts of climate chnage on hydrology in the Yellow River Source region,china. J Water Clim Chang 1–15. https://doi.org/10.2166/wcc.2018.085

Kebede S, Travi Y, Alemayehu T, Marc V (2006) Water balance of Lake Tana and its sensitivity to fluctuations in rainfall, Blue Nile basin, Ethiopia. J Hydrol 316:233–247. https://doi.org/10.1016/j.jhydrol.2005.05.011

Kindu M, Schneider T, Teketay D, Knoke T (2013) Land use/land cover change analysis using object-based classification approach in Munessa-Shashemene landscape of the ethiopian highlands. Remote Sens 5:2411–2435. https://doi.org/10.3390/rs5052411

Knutti R, Masson D, Gettelman A (2013) Climate model genealogy: Generation CMIP5 and how we got there. Geophys Res Lett 40:1194–1199. https://doi.org/10.1002/grl.50256

Knutti R, Sedláček J (2013) Robustness and uncertainties in the new CMIP5 climate model projections. Nat Clim Chang 3:369–373. https://doi.org/10.1038/nclimate1716

Lee S, Yeo I, Sadeghi AM, et al (2018) Comparative analyses of hydrological responses of two adjacent watersheds to climate variability and change using the SWAT model. Hydrol Earth Syst Sci 22:689–708. https://doi.org/doi.org/10.5194/hess-22-689-2018

Lemann T, Roth V, Zeleke G (2017) Impact of precipitation and temperature changes on hydrological responses of small-scale catchments in the Ethiopian Highlands. Hydrol Sci J 62:270–282. https://doi.org/10.1080/02626667.2016.1217415

Li F, Zhang G, Xu YJ (2016) Assessing Climate Change Impacts on Water Resources in the Songhua River Basin. Water 8:1–17. https://doi.org/10.3390/w8100420

Liersch S, Tecklenburg J, Rust H, et al (2018) Are we using the right fuel to drive hydrological models? A climate impact study in the Upper Blue Nile. Hydrol Earth Syst Sci 22:2163–2185. https://doi.org/10.5194/hess-22-2163-2018b

Marhaento H, Booij MJ, Hoekstra AY (2018) Hydrological response to future land-use change and climate change in a tropical catchment. Hydrol Sci J 63:1368–1385. https://doi.org/10.1080/02626667.2018.1511054

Mechal A, Wagner T, Birk S (2015) Recharge variability and sensitivity to climate: The example of Gidabo River Basin, Main Ethiopian Rift. J Hydrol Reg Stud 4:644–660. https://doi.org/10.1016/j.ejrh.2015.09.001

Mekonnen D, Disse M (2018) Analyzing the future climate change of Upper Blue Nile River basin using statistical downscaling techniques. Hydrol Earth Syst Sci 22:2391–2408. https://doi.org/10.5194/hess-22-2391-2018

Melke A, Abegaz F (2017) Impact of climate change on hydrological responses of Gumara catchment, in the Lake Tana Basin - Upper Blue Nile Basin of Ethiopia. Int J Water Resour Environ Eng 9:8–21. https://doi.org/10.5897/ijwree2016.0658

Moriasi DN, Arnold JG, Liew MW Van, et al (2007) Model Evaluation Guidelines for Systematic Quantification of Accuracy in Watershed Simulations. Trans ASABE 50:885–900. https://doi.org/10.1234/590

Nash J, Sutcliffe J (1970) River Flow Forecasting Through Conceptual Models Part 1 - A Discussion of principles. J Hydrol 10:282–290. https://doi.org/10.1080/00750770109555783

Neitsch S., Arnold J., Kiniry J., Williams J. (2011) Soil & Water Assessment Tool Theoretical Documentation Version 2009

Ngongondo C, Li L, Gong L, et al (2013) Flood frequency under changing climate in the upper Kafue River basin, southern Africa: A large scale hydrological model application. Stoch Environ Res Risk Assess 27:1883–1898. https://doi.org/10.1007/s00477-013-0724-z

Nigatu ZM, Rientjes T, Haile AT (2016) Hydrological Impact Assessment of Climate Change on Lake Tana's Water Balance, Ethiopia. Am J Clim Chang 05:27–37. https://doi.org/10.4236/ajcc.2016.51005

Pandey BK, Gosain AK, Paul G, Khare D (2017) Climate change impact assessment on hydrology of a small watershed using semi-distributed model. Appl Water Sci 7:2029–2041. https://doi.org/10.1007/s13201-016-0383-6

Polanco EI, Fleifle A, Ludwig R, Disse M (2017) Improving SWAT model performance in the upper Blue Nile Basin using meteorological data integration and subcatchment discretization. Hydrol Earth Syst Sci 21:4907–4926. https://doi.org/10.5194/hess-21-4907-2017

Roth V, Lemann T, Zeleke G, et al (2018) Effects of climate change on water resources in the upper Blue Nile Basin of Ethiopia. Heliyon 4:1–26. https://doi.org/10.1016/j.heliyon.2018.e00771

Setegn SG, Rayner D, Melesse AM, et al (2011) Impact of climate change on the hydroclimatology of Lake Tana Basin, Ethiopia. Water Resour Res 47:1–13. https://doi.org/10.1029/2010WR009248

Setegn SG, Srinivasan R, Dargahi B (2008) Hydrological Modelling in the Lake Tana Basin, Ethiopia Using SWAT Model. Open Hydrol J 2:49–62. https://doi.org/10.2174/1874378100802010049

Sisay K, Thurnher C, Hasenauer H (2017) Daily climate data for the Amhara region in Northwestern Ethiopia. Int J Climatol 37:2797–2808. https://doi.org/10.1002/joc.4880

Skamarock WC, Klemp JB, Dudhia J, et al (2008) A Description of the Advanced Research WRF Version 3

Smitha PS, Narasimhan B, Sudheer KP, Annamalai H (2018) An improved bias correction method of daily rainfall data using a sliding window technique for climate change impact assessment. J Hydrol 556:100–118. https://doi.org/10.1016/j.jhydrol.2017.11.010

Sunde MG, He HS, Hubbart JA, Urban MA (2018) An integrated modeling approach for estimating hydrologic responses to future urbanization and climate changes in a mixed-use midwestern watershed. J Environ Manage 220:149–162. https://doi.org/10.1016/j.jenvman.2018.05.025

Teklay A, Dile YT, Asfaw DH, et al (2019) Impacts of land surface model and land use data on WRF model simulations of rainfall and temperature over Lake Tana Basin, Ethiopia. Heliyon 5:1–14. https://doi.org/10.1016/j.heliyon.2019.e02469

Teklay A, Dile YT, Setegn SG, et al (2018) Evaluation of static and dynamic land use data for watershed hydrologic process simulation : A case study in Gummara watershed , Ethiopia. Catena 172:65–75. https://doi.org/10.1016/j.catena.2018.08.013

Teklesadik AD, Alemayehu T, van Griensven A, et al (2017) Inter-model comparison of hydrological impacts of climate change on the Upper Blue Nile basin using ensemble of hydrological models and global climate models. Clim Change 141:517–532. https://doi.org/10.1007/s10584-017-1913-4

Thompson G, Field P, Rasmussen R, Hall W (2008) Explicit Forecasts of Winter Precipitation Using an Improved Bulk Microphysics Scheme . Part II : Implementation of a New Snow Parameterization. Mon Weather Rev 136:5095–5115. https://doi.org/10.1175/2008MWR2387.1

Van Griensven A, Ndomba P, Yalew S, Kilonzo F (2012) Critical review of SWAT applications in the upper Nile basin countries. Hydrol Earth Syst Sci 16:3371–3381. https://doi.org/10.5194/hess-16-3371-2012

van Vuuren DP, Edmonds J, Kainuma M, et al (2011) The representative concentration pathways: An overview. Clim Change 109:5–31. https://doi.org/10.1007/s10584-011-0148-z

Wagner PD, Bhallamudi SM, Narasimhan B, et al (2016) Dynamic integration of land use changes in a hydrologic assessment of a rapidly developing Indian catchment. Sci Total Environ 539:153–164. https://doi.org/10.1016/j.scitotenv.2015.08.148

Woldesenbet T, Elagib NA, Ribbe L, Heinrich J (2018) Catchment response to climate and land use changes in the Upper Blue Nile sub-basins, Ethiopia. Sci Total Environ 644:193–206. https://doi.org/10.1016/j.scitotenv.2018.06.198

Worqlul AW, Dile YT, Ayana EK, et al (2018) Impact of climate change on streamflow hydrology in headwater catchments of the upper Blue Nile Basin, Ethiopia. Water 10:1–18. https://doi.org/10.3390/w10020120

Wulong B, Pengfei D, Tie L, et al (2018) Simulating hydrological responses to climate change using dynamic and statistical downscaling methods: a case study in the Kaidu River Basin, Xinjiang, China. J Arid Land 10:905–920. https://doi.org/10.1007/s40333-018-0068-0

Yhang Y Bin, Sohn SJ, Jung IW (2017) Application of Dynamical and Statistical Downscaling to East Asian Summer Precipitation for Finely Resolved Datasets. Adv Meteorol 2017:1–9. https://doi.org/10.1155/2017/2956373

Zhang B, Shrestha NK, Daggupati P, et al (2018) Quantifying the impacts of climate change on streamflow dynamics of two major rivers of the Northern Lake Erie basin in Canada. Sustainability 10:1–23. https://doi.org/10.3390/su10082897

Tables

Table 1. SWAT model parameters subjected to calibration and validation processes.

No.	Paramters	Decription
1	CN2	SCS runoff curve number
2	ALPHA_BF	Base-flow alpha factor
3	GW_DELAY	Groundwater delay
4	GWQMN	Threshold depth of water in the shallow aquifer required for return flow to occur
5	GW_REVAP	Groundwater "revap" coefficient
6	REVAPMN	Threshold depth of water in the shallow aquifer for "revap" to occur
7	RCHRG_DP	Deep aquifer percolation fraction
8	GWHT	Initial groundwater height
9	SOL_AWC	Available water capacity of the soil layer
10	SOL_K	Saturated hydraulic conductivity
11	CH_K2	Effective hydraulic conductivity in main channel alluvium
12	CH_N2	Manning's "n" value for the main channel
13	SURLAG	Surface runoff lag time
14	OV_N	Manning's "n" value for overland flow
15	EPCO	Plant uptake compensation factor
16	ESCO	Soil evaporation compensation factor
17	SLSUBBSN	Average slope length
18	CANMX	Maximum canopy storage

Table 2. The statistical measures of climate variables before bias correction (WRF) and after bias correction (WRF-BC) for the Lake Tana basin from 2010-2015.

Variables	Statistics	Observed	WRF	WRF-BC
Rainfall	Average (mm/day)	3.97	5.53	4.15
	Bias (mm/day)	-	1.56	0.17
	Correlation	-	0.65	0.78
	RMSE (mm/day)	-	5.43	3.88
Maximum temperature (Tmax)	Average (ºC)	26.40	24.98	26.38
	Bias (ºC)	-	-1.42	-0.02
	Correlation	-	0.76	0.89
	RMSE (ºC)	-	2.31	1.04
Minimum temperature (Tmin)	Average (ºC)	12.00	13.45	12.03
	Bias (ºC)	-	1.45	0.03
	Correlation	-	0.60	0.84
	RMSE (ºC)	-	2.12	0.76

Note: WRF=Weather Research Forecasting (WRF) simulation before bias correction, and WRF-BC=Weather Research Forecasting (WRF) simulation after bias correction.

Table 3. Goodness-of-fit statistics for the calibration and validation periods at the four watersheds.

Watersheds	Simulation period	NSE	PBIAS	p-factor	r-factor
Gilgel Abay	Calibration	0.92	-1.1	0.94	0.40
	Validation	0.82	-6.1	0.90	0.65
Gumara	Calibration	0.90	10.1	0.88	0.39
	Validation	0.88	-7.2	0.82	0.61
Ribb	Calibration	0.83	-15.4	0.78	0.60
	Validation	0.75	-8.3	0.76	0.91
Megech	Calibration	0.72	-15.1	0.75	0.59
	Validation	0.77	8.4	0.76	0.80

Table 4. Annual average climate variables and hydrologic components for the baseline and projected period over the study watersheds. AT; Average TemperatureET: Evapotranspiration; and SF: Streamflow.

Variable	Statistics	Gilgel Abay			Gumara			Ribb			Megech		
		Base	RCP4.5	RCP8.5	Base	RCP4.5	RCP8.5	Base	RCP4.5	RCP8.5	Base	RCP4.5	RCP8.5
AT	Average (°C)	17.4	19.1	19.9	18.2	20	20.8	17.6	19.2	20.1	19.8	21.4	22.3
	Change (%)	-	9.4	14.1	-	10	14.5	-	8.9	13.9	-	8.2	12.4
Rainfall	Average (mm)	1928	2354	2597	1525	1585	1862	1589	1680	1864	1169	1200	1202
	Change (%)	-	22.1	34.7	-	3.9	22.1	-	5.7	17.4	-	2.6	2.9
ET	Average (mm)	643	644	712	601	658	700	556	599	625	555	564	604
	Change (%)	-	0.1	10.7	-	9.6	16.5	-	7.8	12.5	-	1.7	8.9
SF	Average (mm)	857	1190	1356	883	884	1119	528	549	672	217	255	238
	Change (%)	-	38.9	58.2	-	0.1	26.7	-	4.0	27.3	-	17.5	9.7

Figures

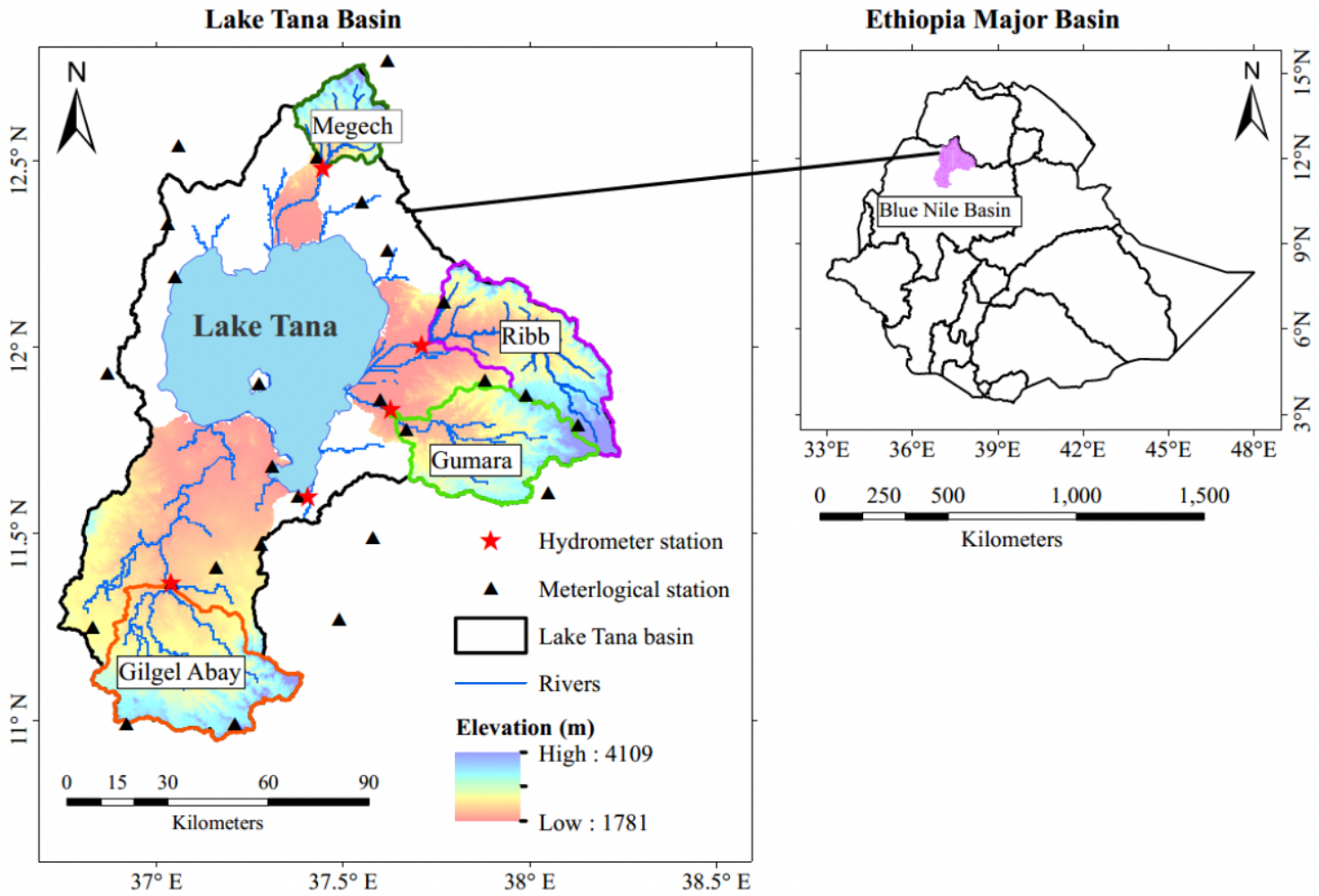

Figure 1

The Lake Tana basin showing its four major watersheds (Gilgel Abay, Gumara, Ribb, and Megech river), streamflow and climate gauging stations with Digital Elevation Model (DEM) as a background. The map in the left shows the Ethiopian 12 major river basins.

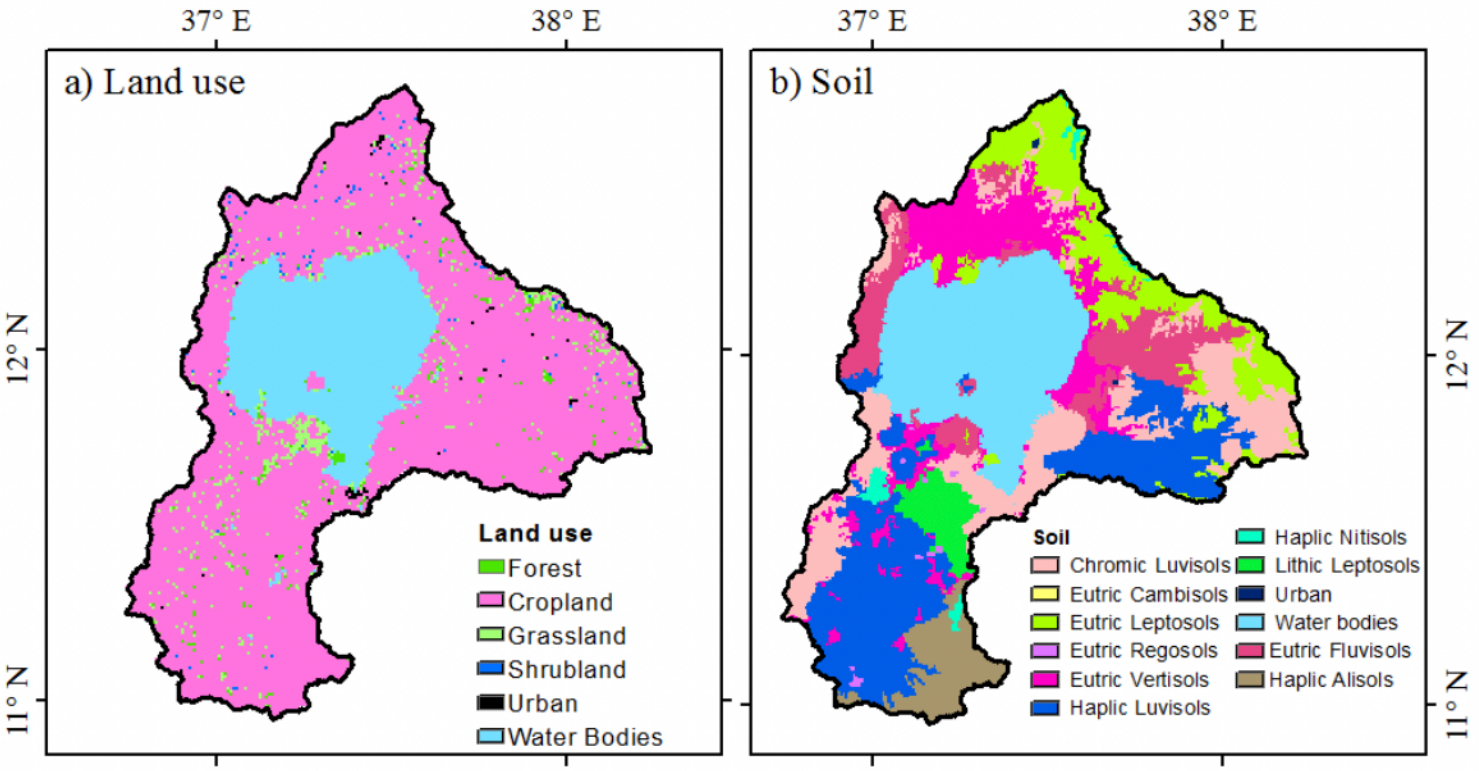

Figure 2

Lake Tana basin land use and soil map subjected to hydrological model simulation.

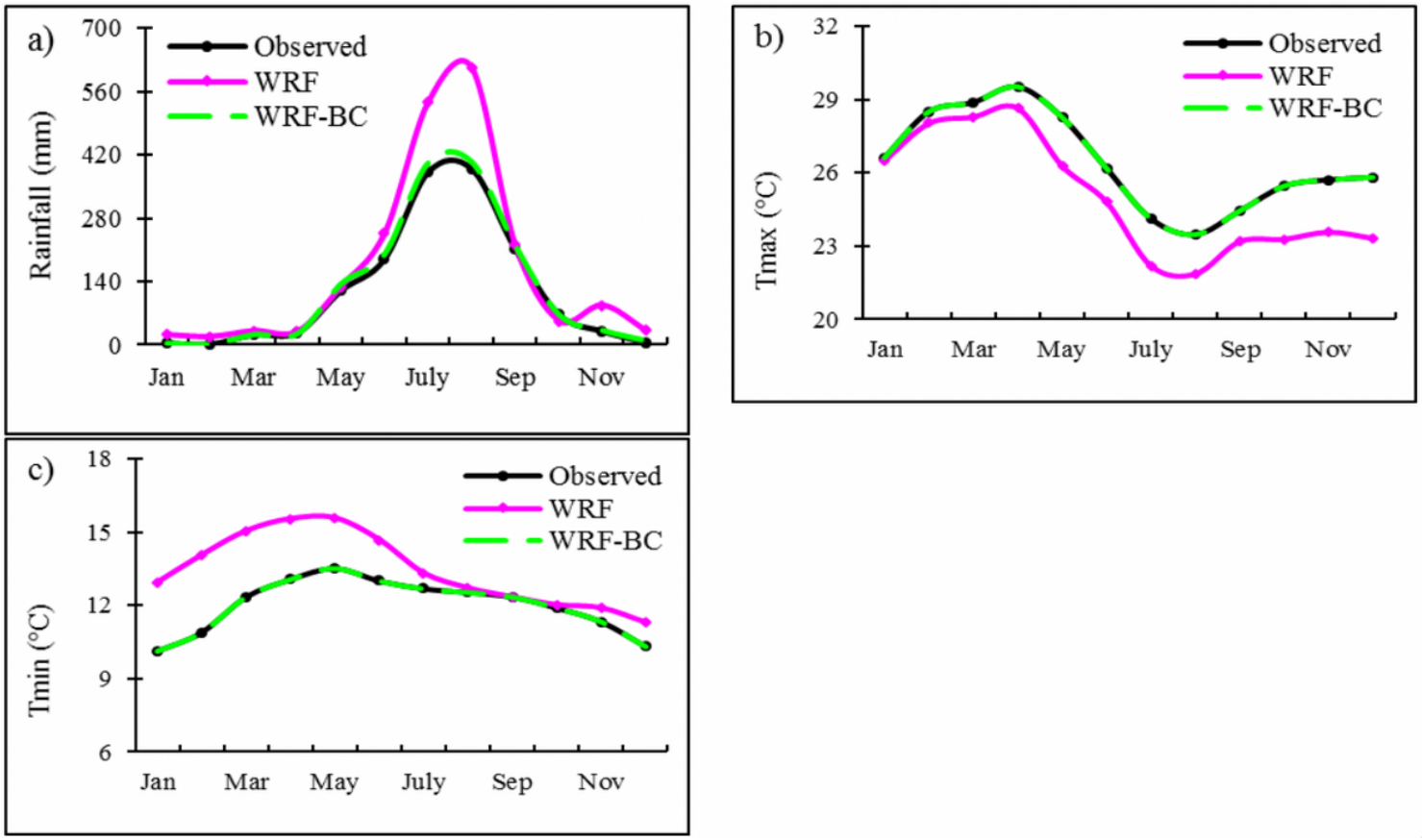

Figure 3

Monthly mean observed and WRF simulated (before and after bias correction) rainfall (a), maximum temperature (b), and minimum temperature (c) from the Lake Tana basin during 2010-2015. WRF and WRF-BC represent model simulations before and after bias correction, respectively.

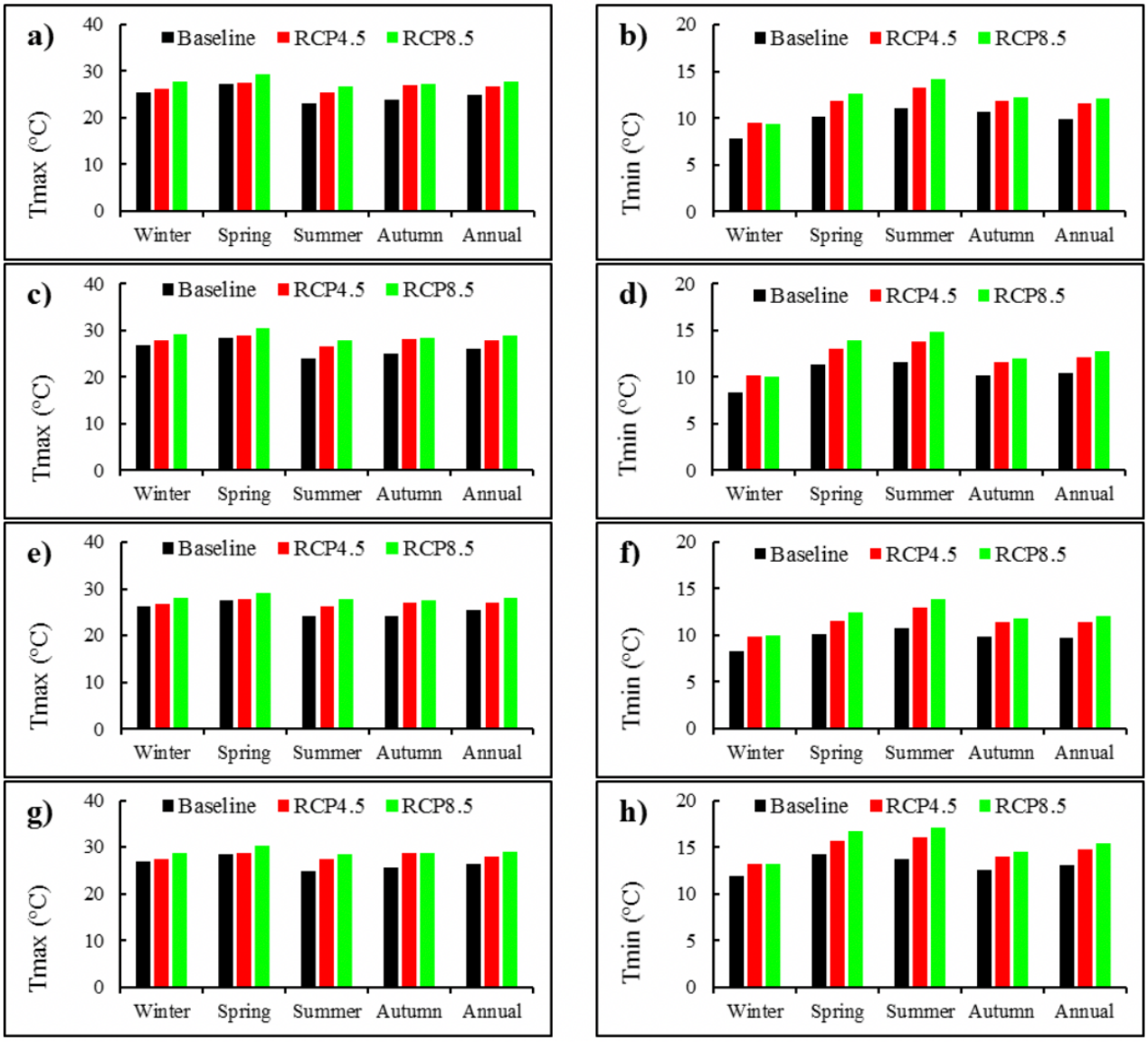

Figure 4

Seasonal and annual maximum temperature (a, c, e, and g) and minimum temperature (b, d, f, and h) in the Gilgel Abay watershed (a and b); Gumara watershed (c and d); Ribb watershed (e and f); and Megech watershed (g and h) in the Lake Tana basin.

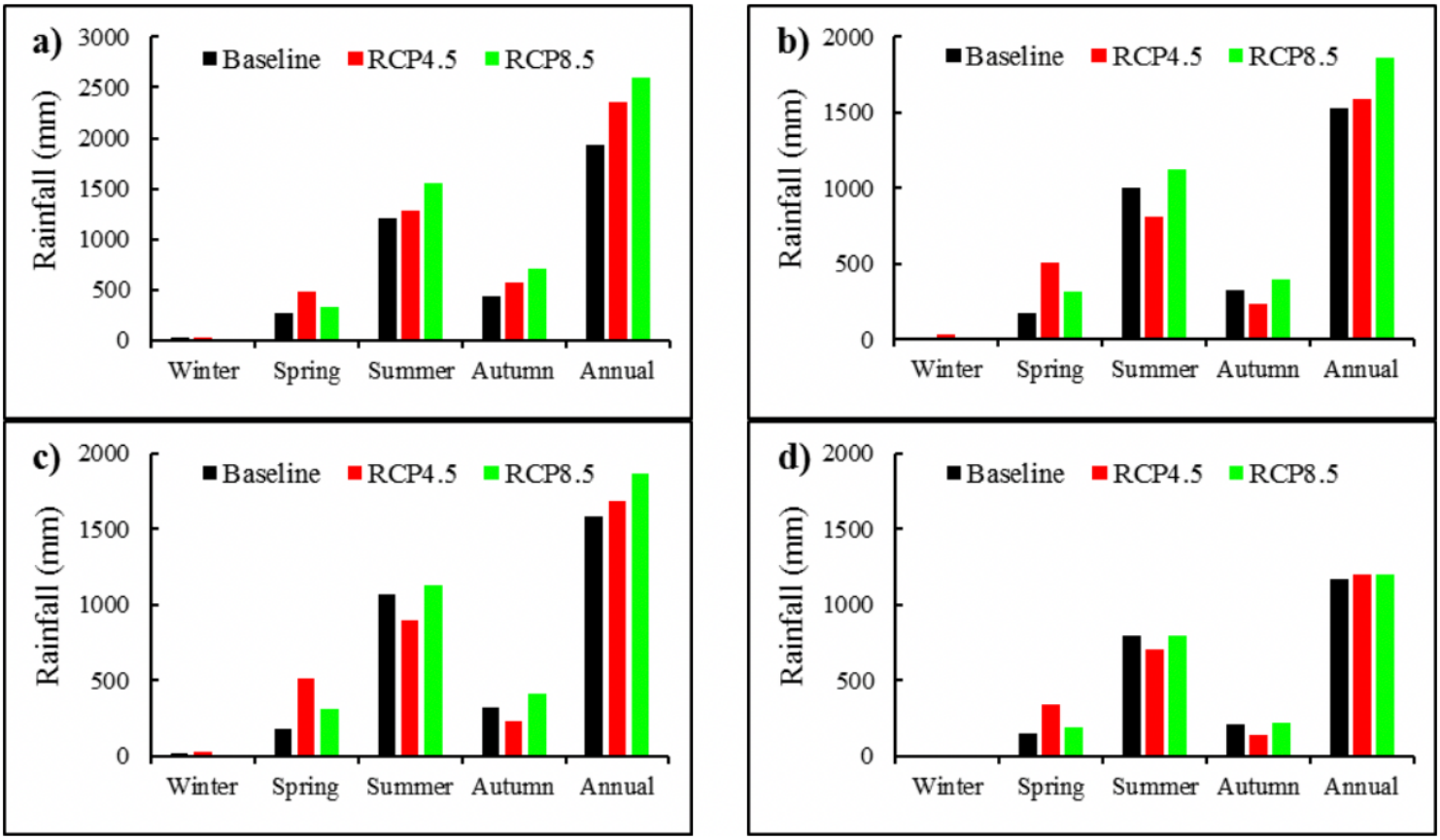

Figure 5

The seasonal and mean annual rainfall distribution in the Gilgel Abay watershed (a); Gumara watershed (b); Ribb watershed (c); and Megech watershed (d).

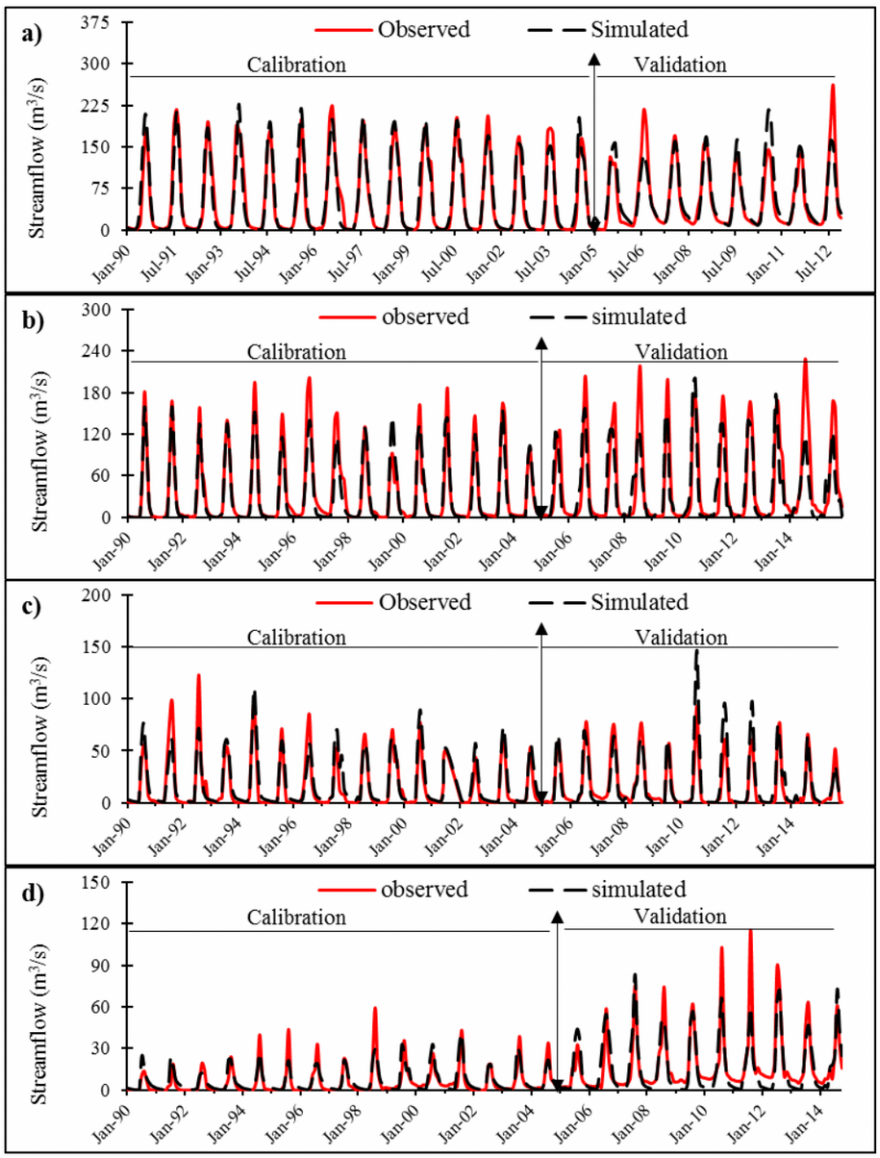

Figure 6

Observed and simulated monthly streamflow for the calibration (1990-2004) and validation period (2005-2015) at; a) Gilgel Abay, b) Gumara, c) Ribb, and d) Megech watershed.

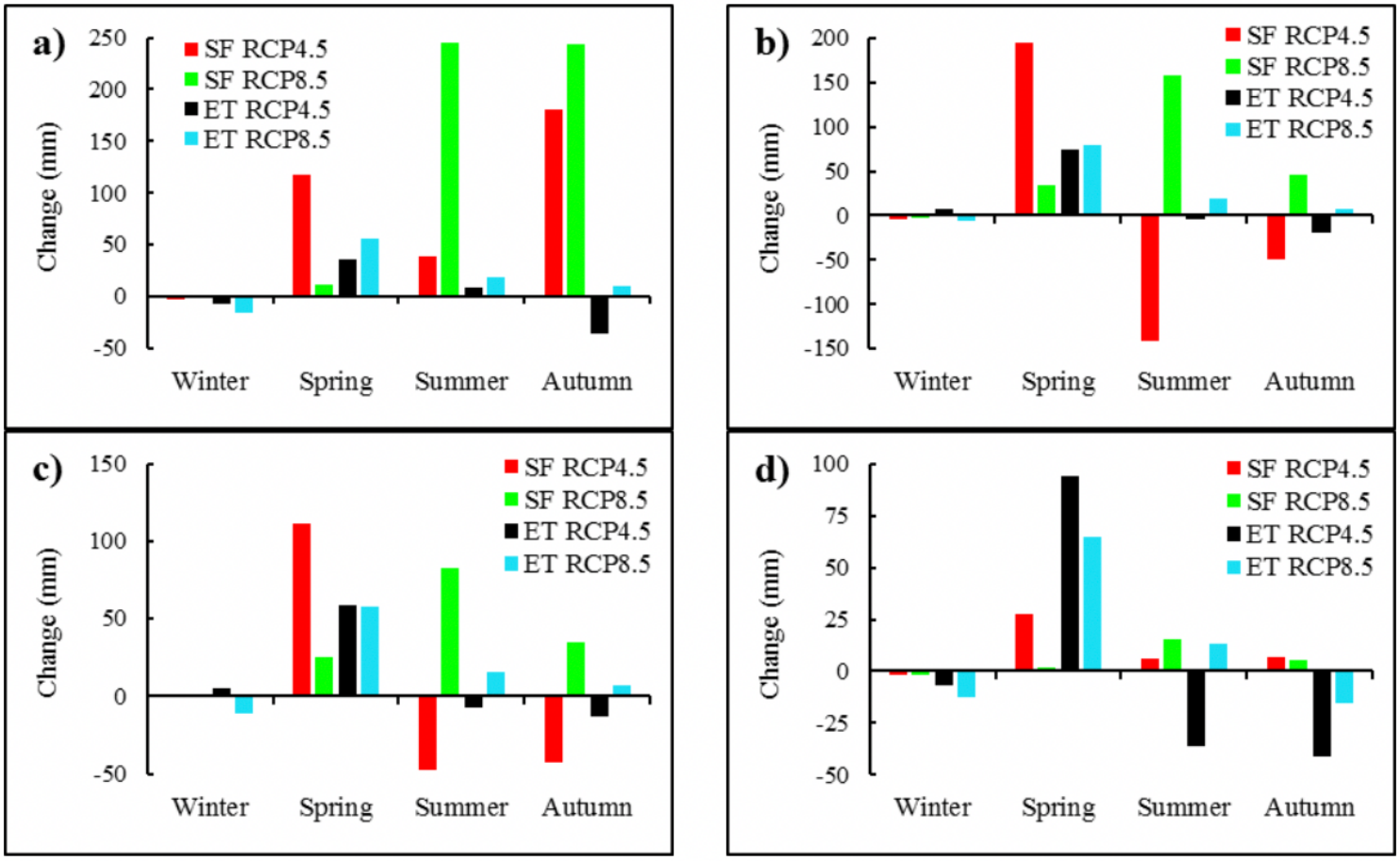

Figure 7

The projected (2046-2051) seasonal streamflow (SF) and evapotranspiration (ET) percentage of changes relative to the baseline period (2010-2015) at: (a) Gilgel Abay, (b) Gumara, (c) Ribb, and (d) Megech watershed.